Title

Spontaneous and photosensitization-induced mutations in primary mouse cells transitioning through senescence and immortalization

Journal

Journal of Biological Chemistry, 295(29)

ISSN

0021-9258

Authors

Caliri, Andrew W

Tommasi, Stella

Bates, Steven E

et al.

Publication Date

2020-07-01

DOI

10.1074/jbc.ra120.014465

Peer reviewed

Spontaneous and photosensitization-induced mutations in primary mouse cells transitioning through senescence and immortalization

Received for publication, May 19, 2020, and in revised form, June 2, 2020 Published, Papers in Press, June 2, 2020, DOI 10.1074/jbc.RA120.014465

Andrew W. Caliri[1], **Stella Tommasi**[1], **Steven E. Bates**[2,†], **and Ahmad Besaratinia**[1,*]

From the [1]*Department of Preventive Medicine, USC Keck School of Medicine, University of Southern California, Los Angeles, California, USA and* [2]*Department of Cancer Biology, Beckman Research Institute of the City of Hope, Duarte, California, USA*

Edited by Patrick Sung

To investigate the role of oxidative stress–induced DNA damage and mutagenesis in cellular senescence and immortalization, here we profiled spontaneous and methylene blue plus light–induced mutations in the *cII* gene from λ phage in transgenic mouse embryonic fibroblasts during the transition from primary culture through senescence and immortalization. Consistent with detection of characteristic oxidized guanine lesions (8-oxodG) in the treated cells, we observed significantly increased relative *cII* mutant frequency in the treated pre-senescent cells which was augmented in their immortalized counterparts. The predominant mutation type in the treated pre-senescent cells was G:C→T:A transversion, whose frequency was intensified in the treated immortalized cells. Conversely, the prevailing mutation type in the treated immortalized cells was A:T→C:G transversion, with a unique sequence-context specificity, *i.e.* flanking purines at the 5′ end of the mutated nucleotide. This mutation type was also enriched in the treated pre-senescent cells, although to a lower extent. The signature mutation of G:C→T:A transversions in the treated cells accorded with the well-established translesion synthesis bypass caused by 8-oxodG, and the hallmark A:T→C:G transversions conformed to the known replication errors because of oxidized guanine nucleosides (8-OHdGTPs). The distinctive features of photosensitization-induced mutagenesis in the immortalized cells, which were present at attenuated levels, in spontaneously immortalized cells provide insights into the role of oxidative stress in senescence bypass and immortalization. Our results have important implications for cancer biology because oxidized purines in the nucleoside pool can significantly contribute to genetic instability in DNA mismatch repair–defective human tumors.

Malignant transformation is a complex multistep process during which genetic, epigenetic, and/or environmental factors trigger a cascade of events, disrupting critical cellular and subcellular targets (1, 2). Of these, disruption of key cell growth regulatory pathways, resulting in uncontrolled cell proliferation, is an early event and a hallmark of carcinogenesis (1, 3). Abrogation of cell-cycle checkpoint controls during malignant transformation releases the cells from senescence, a state of permanent growth arrest without undergoing programmed cell death (apoptosis) (4). Evasion of cellular senescence gives rise to an "indefinite" cell proliferation state, otherwise known as immortalization (5). Immortalization allows cells to continually divide and accumulate additional oncogenic alterations, which may lead to a fully malignant phenotype (3, 5). Understanding the underlying mechanisms of cellular senescence bypass and immortalization can fundamentally improve our knowledge of cancer biology (5).

Cellular senescence, first described by Hayflick in 1961 (6), is a stress condition in which cells, despite being alive, cease to further proliferate (4). Normal adult somatic mammalian cells capable of dividing *in vivo* exhibit a limited life span *in vitro* as they undergo senescence after successive rounds of replication (5). At variable frequency, however, cultivated cells may escape senescence and become immortalized (5, 7). The immortalization frequency seems to be primarily species-dependent (4, 7). Whereas rodent cells efficiently undergo spontaneous immortalization *in vitro*, primary human and avian cells rarely, if ever, become spontaneously immortalized in culture (4, 5). Although the overwhelming majority of cultured rodent cells eventually senesce, few may grow past this barrier, also known as the "crisis" phase, and acquire the ability to grow indefinitely and become immortalized cell lines (5).

Mouse embryonic fibroblasts (MEF) are a classic model system to study replicative senescence and immortalization (5, 8). Primary MEF, grown in standard cell culture conditions and passaged serially, typically undergo senescence after several rounds of passaging, remain in the "crisis" phase for a while, then override the senescence block, re-enter the cell cycle, and switch to an immortalized phenotype (9). It is widely believed that prolonged exposure of cells to supraphysiological concentrations of atmospheric oxygen (20%) used in standard cell culture incubators is a main contributor to senescence and immortalization (10). The nonphysiological O_2 tension, which imposes a significant burden of oxidative stress on the cells, leads to generation of reactive oxygen species (ROS) that induce promutagenic DNA damage, among other macromolecular changes, such as epigenetic modifications (8, 9). The ROS-induced genetic mutations and epigenetic alterations in key genes involved in cell-cycle checkpoints and related regulatory pathways are thought to play a crucial role in senescence bypass and spontaneous immortalization of MEF (3–5, 10).

Transgenic Big Blue® MEF represent a versatile system for studying mutagenesis and immortalization simultaneously

†Deceased.
* For correspondence: Ahmad Besaratinia, besarati@med.usc.edu.

(11, 12). The genome of Big Blue® MEF contains multiple copies of the chromosomally integrated, and easily recoverable, λLIZ shuttle vector, which carries two mutation reporter genes, namely the *LacI* and *cII* transgenes (11). In the present study, we have constructed a comprehensive catalogue of spontaneous and photosensitization-induced mutations in a mammalian genome by interrogating the *cII* gene from λ phage in transgenic Big Blue® MEF during the transition from primary culture through senescence and immortalization. More specifically, we have determined the mutant frequency of *cII* transgene as well as characterized the spectra of *cII* mutation in Big Blue® MEF treated with methylene blue plus visible light and counterpart untreated cells both before senescence and after immortalization. Methylene blue is a photosensitizer that, upon excitation with visible light, produces reactive oxygen species (mainly singlet oxygen ($^1O_2$)) which primarily cause oxidation of purine and pyrimidine bases in the DNA, with oxidized guanine residues, such as 8-oxo-7,8-dihydro-2′-deoxyguanosine (8-oxodG), being the predominant and highly mutagenic lesion (13–15). To verify the effectiveness of methylene blue plus light treatment in inducing promutagenic DNA damage *in vitro*, we subjected the genomic DNA of the treated and untreated cells to enzymatic digestion with formamidopyrimidine DNA glycosylase (Fpg), which cleaves 8-oxodG and other oxidized/ring-opened purines (16, 17), followed by visualization with alkaline gel electrophoresis. A flowchart of the study is shown in Fig. 1.

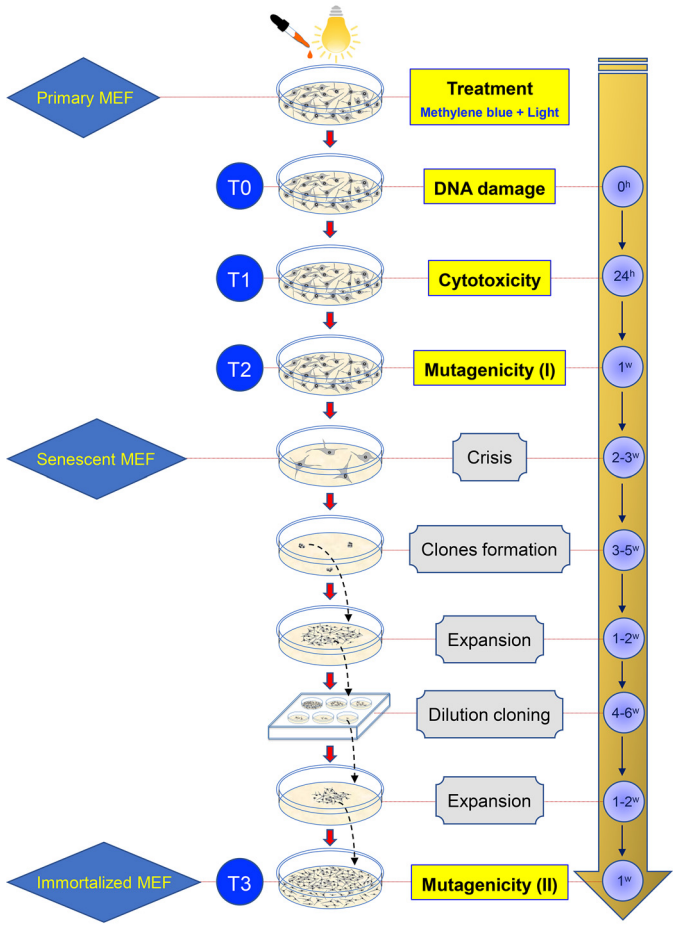

Figure 1. Flow chart of the study design. *T0*, immediately after methylene blue plus light treatment, cells were used for DNA damage analysis. *T1*, 24 h posttreatment (primary MEF), cells were used for cytotoxicity examination. *T2*, 8 days posttreatment (early passage pre-senescent MEF), cells were used for the first mutagenicity analysis. *T3*, cells were used for the second mutagenicity analysis (immortalized MEF).

Results

Cytotoxicity examination

As shown in Fig. 2*A*, treatment of MEF with methylene blue plus light was dose-dependently cytotoxic. Dependent on both the concentration of methylene blue and the duration of light exposure, cell viability decreased as the administered dose increased. Treatment with 2 μM methylene blue plus 5 min light exposure resulted in 80.0 ± 2.7% cell viability that met the threshold limit of cytotoxicity set for our mutagenicity experiments. Higher doses of methylene blue plus light were prohibitively cytotoxic as they caused high to excessive cell death in the treated MEF (Fig. 2*A*). As indicated earlier, moderate to high cell survival post treatment is optimal and most amenable for mutagenicity studies (12, 18, 19). We also note that methylene blue treatment alone or light exposure only at the tested conditions did not cause any detectable cytotoxicity in MEF (data not shown).

DNA damage detection

Primary MEF treated with methylene blue plus light showed dose-dependent formation of oxidative DNA damage as illustrated by increasing levels of Fpg-sensitive sites, which are indicative of 8-oxodG and other oxidized/ring-opened purines (16, 17), in the genomic DNA of the treated cells (Fig. 2*B*). The extent of the induced DNA damage was directly related to both the concentration of methylene blue and the length of light exposure. As shown in Fig. 2*B*, a substantial and readily detectable level of oxidative DNA damage was observed in cells treated with 2 μM methylene blue plus 5 min light exposure. Consistent with the cytotoxicity results (above), this observation ensured that such treatment is effective in inducing promutagenic DNA damage for our mutagenicity experiments.

Mutation analysis

To investigate the role played by oxidative stress–induced DNA damage and mutagenesis in cellular senescence and immortalization, we have determined the *cII* mutant frequency and mutation spectrum in Big Blue® MEF treated with methylene blue plus light and counterpart untreated cells both before senescence (T2) and after immortalization (T3). Based on the cytotoxicity and DNA damage results, we selected 2 μM methylene blue treatment plus 5 min light exposure for the mutagenicity experiments. Table 1 summarizes the *cII* mutant frequency data for the treated and control cells before senescence (at T2) and after immortalization (at T3). As shown in Table 1, the *cII* mutant frequencies were significantly increased in the treated cells relative to controls both before senescence (13.6 ± 2.5 *versus* 5.2 ± 1.3 × 10^{-5}, $p = 0.0326$) and after immortalization (50.8 ± 6.8 *versus* 9.3 ± 1.8 × 10^{-5}, $p = 0.002$). More specifically, there were 2.6-fold and 5.4-fold increases in relative *cII* mutant frequencies in the treated cells at T2 and T3, respectively (*versus* counterpart controls). In both the treated and

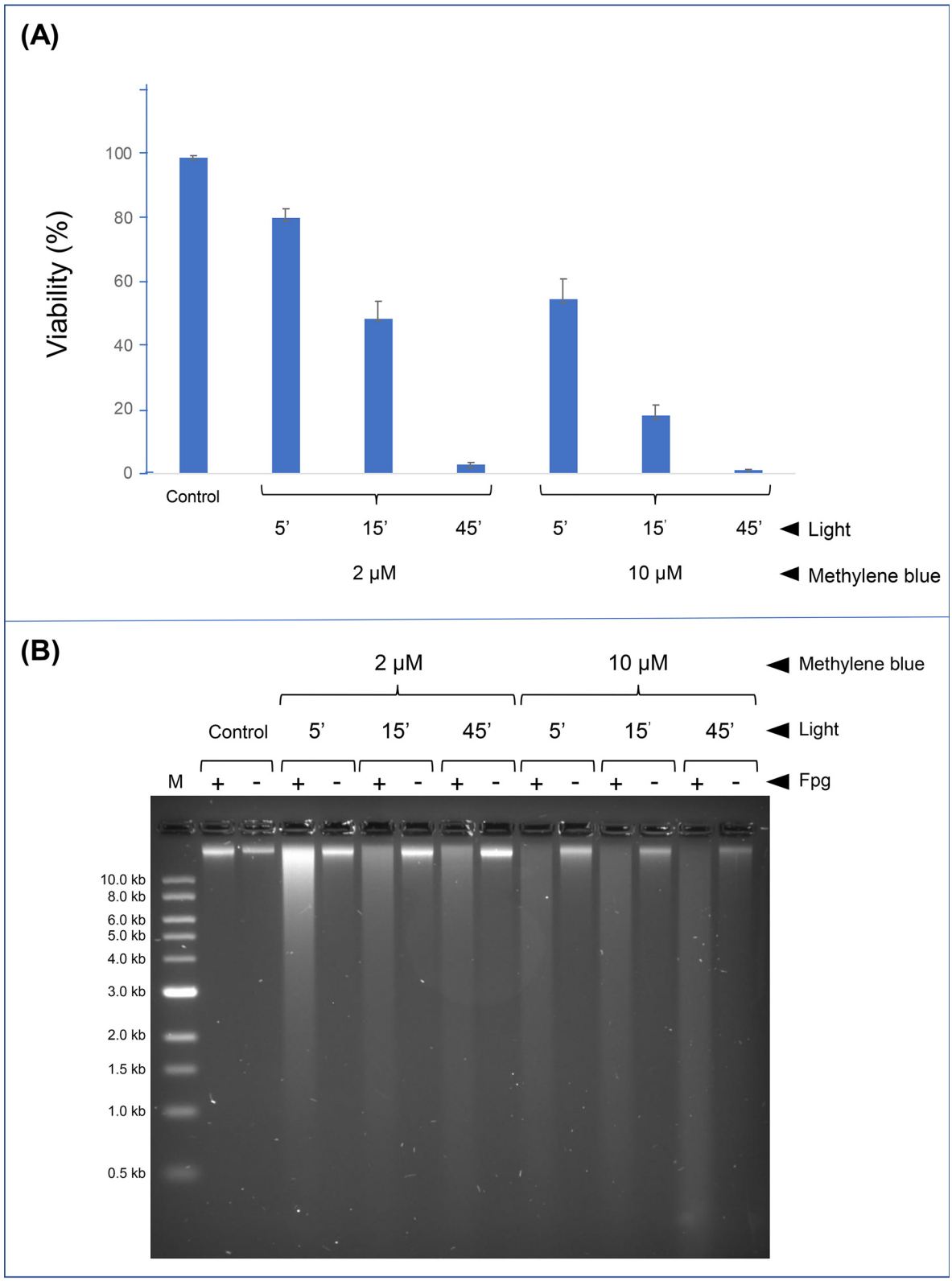

Figure 2. Detection of cytotoxicity and DNA damage in Big Blue® MEF treated with methylene blue plus light and counterpart untreated cells. *A*, cytotoxicity examination was performed by the trypan blue dye exclusion technique, as described in the text. The percentage of viable cells was determined in triplicate cultures prepared for each treatment condition, and the results were expressed as median ± S.E. *B*, oxidative DNA damage was detected by digestion of the genomic DNA with Fpg enzyme, followed by visualization with alkaline gel electrophoresis, as described in the text. (+) and (−) represent the presence and absence, respectively, of Fpg enzyme in the reaction mix. M = molecular size marker.

Table 1

***cII* Mutant frequency in Big Blue® MEF treated with methylene blue plus light and counterpart untreated cells before senescence (T2) and after immortalization (T3)**

Sample	Total screened plaques (pfu*)	Putative *cII* mutant plaques	Verified *cII* mutant plaques (re-plated)†	Reconfirmed *cII* mutant plaques (sequenced)†	Adjusted *cII* mutant frequency ($\times 10^{-5}$)‡
Control (T2)	1,375,000	151	114	79	5.2 + 1.3
Control (T3)	1,215,020	162	149	126	9.3 + 1.8
Methylene blue + light (T2)	1,029,300	171	140	129	13.6 + 2.5§
Methylene blue + light (T3)	401,511	176	165	164	50.8 + 6.8¶#

*Plaque forming unit.
†Putative *cII* mutant plaques were first re-plated for verification and then sequenced for reconfirmation.
‡The *cII* mutant frequency was adjusted based on the total number of plaques that were first verified by re-plating and then reconfirmed by DNA sequencing. Samples from each group were assayed for five to eight times and the results are expressed as median ± S.E.
§Statistically significant *versus* control (T2).
¶Statistically significant *versus* control (T3).
#Statistically significant *versus* methylene blue + light (T2).

Table 2

Types of mutation in the *cII* gene in Big Blue® MEF treated with methylene blue plus light and counterpart untreated cells before senescence (T2) and after immortalization (T3)

Mutation type	Control (T2)	Control (T3)	Methylene blue + light (T2)	Methylene blue + light (T3)
Single mutation	75 (94.9%)	121 (96.0%)	129 (100.0%)	162 (98.8%)
Multiple mutations	4 (5.1%)	5 (4.0%)	0 (0.0%)	2 (1.2%)
Base substitution	79 (95.2%)	126 (96.2%)	124 (96.1%)	159 (95.8%)
Indel				
Insertion	3 (3.6%)	3 (2.3%)	2 (1.6%)	0 (0.0%)
Deletion	1 (1.2%)	2 (1.5%)	3 (2.3%)	7 (4.2%)

Percentages are indicated in brackets.

control cells, the *cII* mutant frequencies were higher at T3 than T2; in the immortalized treated and control cells, respectively, the *cII* mutant frequencies were 3.4-fold and 1.8-fold higher than those in the corresponding pre-senescent cells ($p = 0.0079$ and $p = 0.06527$, respectively).

To establish the mutation spectra of the *cII* gene in the treated and control cells before senescence and after immortalization, we performed direct DNA sequencing on the mutant plaques detected in the respective samples. We sequenced 140 and 165 putative mutant plaques from the pre-senescent and immortalized treated cells, respectively, and 114 and 149 plaques from the corresponding control cells. Of these, 129, 164, 79, and 126, respectively, had a minimum of one mutation in the *cII* gene, as detected by DNA sequencing. This is well within the historical range for the *cII* assay because in the Big Blue® λLIZ system, WT *cII*-bearing phages with a mutation in the *cI* gene can also give rise to a phenotypically expressed mutant plaque (11, 12, 20). Table 2 is a compilation of data on the types of mutation found in the *cII* gene in the treated and control cells before senescence (T2) and after immortalization (T3). In all cases, single base substitutions composed the overwhelming majority of the detected *cII* mutations, *i.e.* 96.1 and 95.8% in the treated cells at T2 and T3, respectively, and 95.2 and 96.2% in the corresponding control cells. The remainder mutations were almost exclusively single insertions or deletions (Table 2).

To compare and contrast the frequency distribution of mutations detected in the *cII* gene in the treated and control cells before senescence and after immortalization, we calculated the frequency of each specific type of mutation (*e.g.* transition, transversion, indel) in the respective groups. The frequency of each type of mutation in a group was determined by multiplying the percentage of its occurrence to the *cII* mutant frequency of the corresponding group. As shown in Fig. 3*A*, the frequency distribution of the induced *cII* mutations in the treated cells both at T2 and T3 differed from those in the respective controls; of note, the differences were mostly augmented at T3. There were statistically significant increases in frequencies of G:C→T:A transversions (8.9-fold), A:T→G:C transitions (3.6-fold), A:T→C:G transversions (2.8-fold), indels (2.1-fold), and G:C→A:T transitions (1.6-fold) in the treated cells at T2 (pre-senescent) relative to respective controls (Fig. 3*B*). The treated cells at T3 (immortalized) showed statistically significant rises in frequencies of A:T→C:G transversions (23.0-fold), G:C→C:G transversions (13.7-fold), G:C→T:A transversions (11.3-fold), indels (8.6-fold), G:C→A:T transitions (2.7-fold), and A:T→G:C transitions (2.1-fold) relative to pre-senescent controls. The immortalized control cells (at T3) also showed higher frequencies of G:C→T:A transversions and A:T→T:A transversions (3.3-fold), and G:C→C:G transversions (2.4-fold) relative to pre-senescent control cells (at T2) (Fig. 3*B*).

Furthermore, we constructed a detailed map of the location and type of mutations detected in the *cII* gene in the treated and control cells before senescence and after immortalization. As shown in Fig. 4, single or recurring mutations were found at various nucleotide positions along the *cII* gene in the treated and control cells both at T2 and T3. We also performed sequence-context analysis on the detected mutations in the treated and control cells before senescence and after immortalization. Mutations occurring at A:T base pairs were more frequent in the immortalized treated cells than counterpart controls ($p = 0.0162$) and pre-senescent treated cells ($p = 0.0217$) (Fig. 5*A*). Mutations within CpG-containing sequences were proportionally similar across the treated and control cells (both at T2 and T3) (Fig. 5*B*). However, G:C→A:T transitions at CpG dinucleotides, which are attributed to spontaneous deamination of 5-methylcytosine (21), were slightly overrepresented in the pre-senescent and immortalized control cells relative to respective treated cells (Fig. 5*C*). Of importance, all CpGs within the *cII* gene are heavily methylated (11). The most frequent type of mutation in the immortalized treated cells, A:T→C:G transversions, occurred almost exclusively at a sequence context in which the mutated nucleotide was preceded, at the 5′ end, by a purine residue (98.7%), predominantly adenine

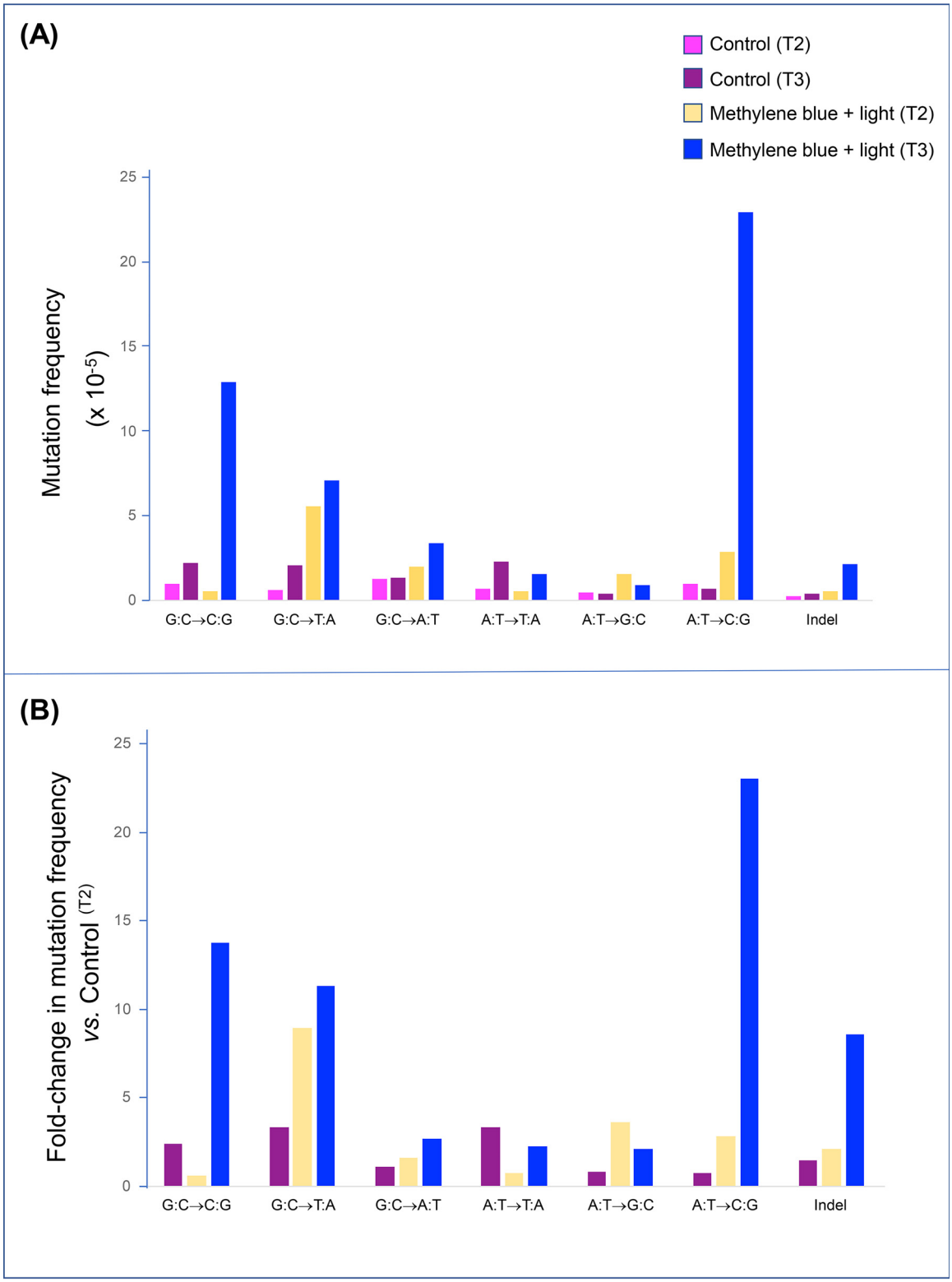

Figure 3. Frequency distribution of mutations in the *cII* gene in Big Blue® MEF treated with methylene blue plus light and counterpart untreated cells before senescence (T2) and after immortalization (T3). *A*, frequency of each specific type of mutation (*e.g.* transition, transversion, indel) was determined in the treated and control cells. The frequency of each type of mutation in a group was calculated by multiplying the percentage of its occurrence to the *cII* mutant frequency of the corresponding group. indel = insertion + deletion. *B*, -fold changes in frequency of each specific type of mutation in the treated cells (at T2 and T3) and control cells (at T3) relative to background in control cells at T2 are shown. -Fold change represents the frequency of a specific type of mutation in a group divided by the frequency of the same type of mutation in control at T2.

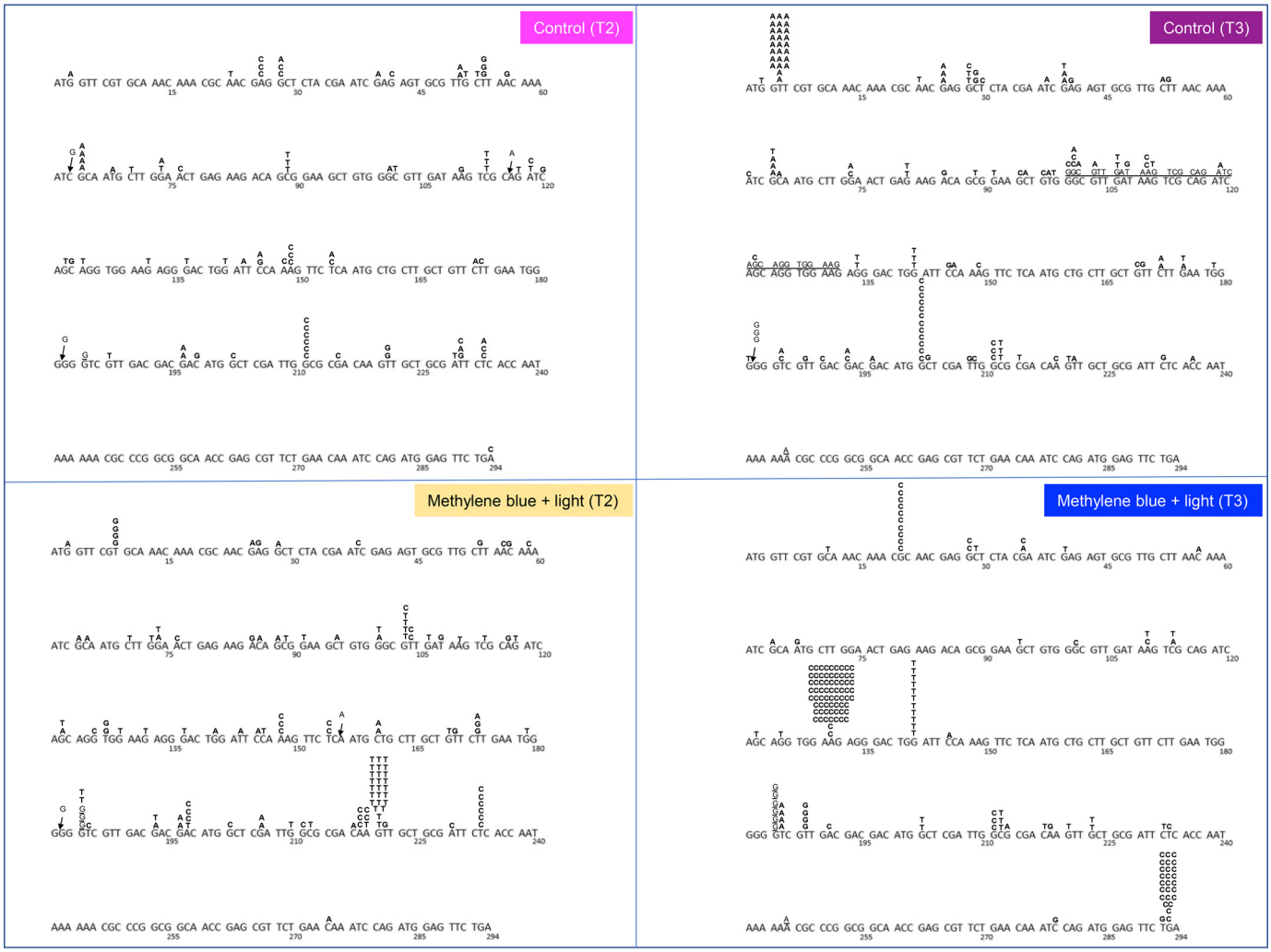

Figure 4. Detailed map of the location and type of mutations detected in the *cII* gene in Big Blue® MEF treated with methylene blue plus light and counterpart untreated cells before senescence (T2) and after immortalization (T3). The detected mutations in each group were plotted against the reference *cII* sequence. Mutated bases are typed above the reference sequence. Deleted bases are *underlined*; multiple deletions are continuously *underlined*. Inserted bases are shown with an *arrow*. *Numbers* below the reference bases denote the corresponding nucleotide positions in the *cII* sequence.

(Fig. 5*D*). This unique sequence specificity of A:T→C:G transversions in the immortalized treated cells was most distinguishable at nucleotide position 131 in the *cII* gene, which represents a mutational hotspot.

Discussion

In the present study, MEF treated with methylene blue plus light and counterpart untreated cells entered senescence within days of each other, and stayed at the crisis phase for approximately the same duration of time, although resumption of robust growth post crisis was slightly faster in the treated cells. Upon emergence from senescence, all the treated and control cultures formed multiple single-cell colonies that were subsequently expanded to generate independent immortalized cell lines. As shown in Table 1, treatment with methylene blue plus light was significantly mutagenic to Big Blue® MEF both at the pre-senescent (T2) and immortalized (T3) stages; however, the extent of mutagenicity was higher at T3 than T2. This was reflected by the 5.4-fold and 2.6-fold increases in relative *cII* mutant frequencies in the treated cells at T3 and T2, respectively (*versus* counterpart controls). Of note, untreated control cells that had undergone spontaneous immortalization, also showed elevated frequency of *cII* mutants relative to pre-senescent control cells (1.8-fold increase) (Table 1).

Photosensitization of methylene blue with visible light generates predominantly $^1O_2$ through a type II reaction in which the excited methylene blue in a triplet state transfers energy to ground state molecular oxygen (13–15). $^1O_2$ interacts preferentially with guanine moiety in DNA to form 8-oxodG and, less frequently, other oxidized/ring-opened purines, such as 2,6-diamino-4-hydroxy-5-formamidopyrimidine (FapyG) (17). The induced DNA lesions are all substrates for Fpg, a base excision repair enzyme (16, 22, 23). Methylene blue in the triplet excited state may partly react with DNA through a type I photosensitization reaction, which involves preferential oxidation of guanine, and formation of 8-oxodG and, to a lesser extent, FapyG (15, 24). The preferential targeting of guanine by $^1O_2$ and other ROS is ascribed to the electron-rich nature of this base as it has the lowest oxidation potential of the four DNA bases (25).

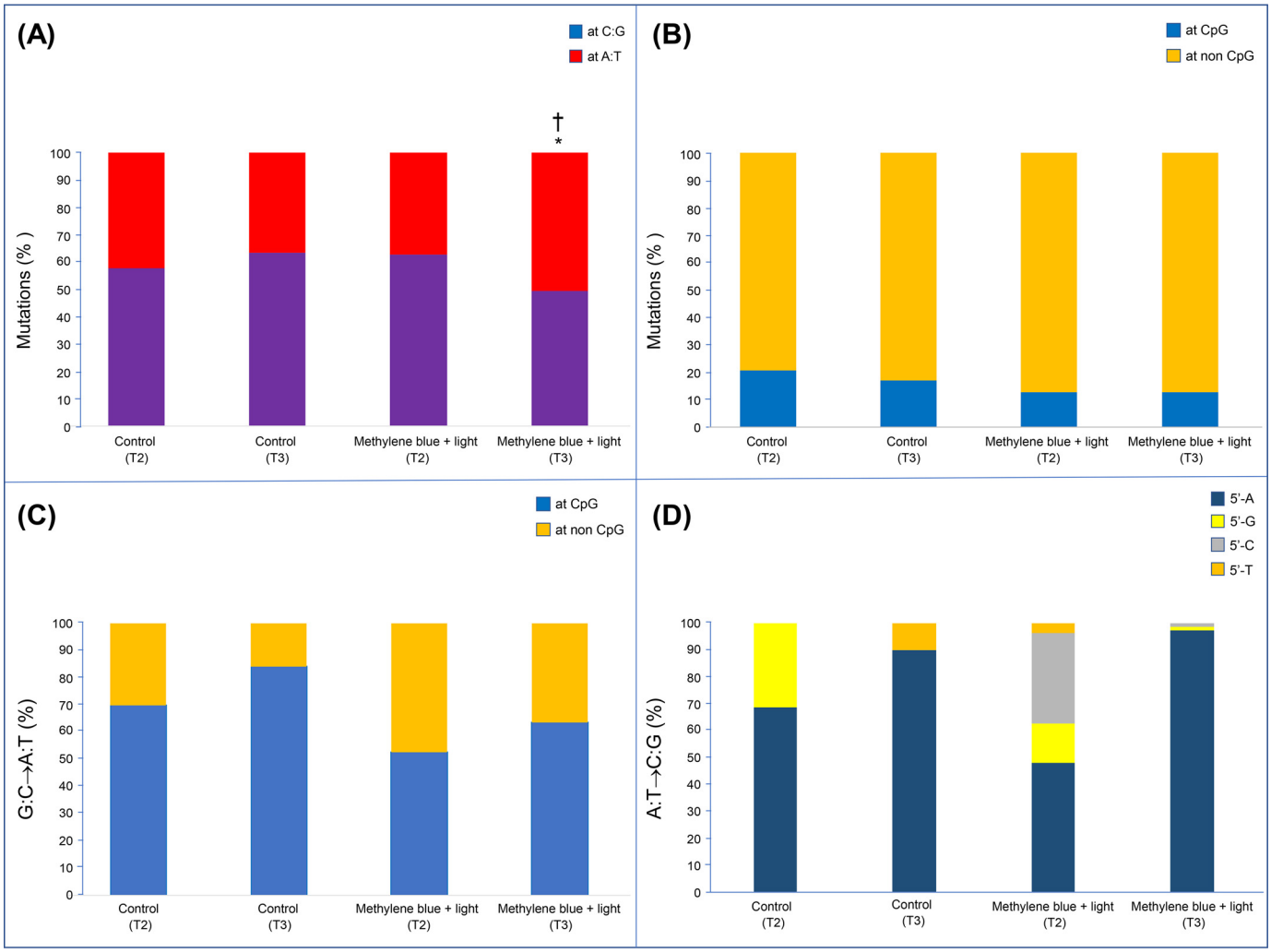

Figure 5. Sequence-context analysis of the detected mutations in the *cII* gene in Big Blue® MEF treated with methylene blue plus light and counterpart untreated cells before senescence (T2) and after immortalization (T3). *A*, distribution of all mutations occurred at A:T *versus* C:G base pairs (*, statistically significant *versus* control (T3), $P = 0.0162$ and †, statistically significant *versus* methylene blue plus light (T2), $P = 0.0217$). *B*, distribution of all mutations occurred at CpG dinucleotides. *C*, distribution of G:C→A:T transitions occurred at CpG dinucleotides. *D*, distribution of bases flanking the 5′ end of the mutated nucleotide in A:T→C:G transversions.

Consistent with the known photochemical properties of methylene blue, we detected extensive formation of Fpg-sensitive sites in the genomic DNA of methylene blue plus light-treated cells, as shown in Fig. 2*B*.

8-oxodG is a miscoding lesion during DNA replication (26, 27). As such, an adenine is preferentially incorporated opposite 8-oxodG in the template DNA during translesion synthesis, which upon next round of DNA replication, produces G:C→T:A transversion (26–28). Treatment of bacteriophage DNA with photoactivated methylene blue has been shown to induce G:C→T:A transversion as a signature mutation in *Escherichia coli* (27, 28). Also, the mutM mutY mutants of *E. coli* deficient in the repair of 8-oxodG:A mispair, have exhibited extremely high rate of spontaneous G:C→T:A transversions (29). In the present study, the most prevalent type of mutation detected in the pre-senescent treated cells was G:C→T:A transversions (Fig. 3*A*). Of significance, this signature mutation was intensified in the immortalized treated cells (Fig. 3*B*). G:C→T:A transversions were also overrepresented in the immortalized control cells relative to pre-senescent counterparts (*i.e.* 3.3-fold increase in relative frequency; Fig. 3*B*).

Although 8-oxodG predominantly induces G:C→T:A transversion (26–28), bypass of this lesion in mammalian cells can also lead to G:C→A:T transition and G:C→C:G transversion (30, 31). The latter types of mutation presumably arise from further photooxidation of 8-oxodG, resulting in hydantoin-type lesions (32). In our study, G:C→A:T transitions were enriched in the pre-senescent treated cells, and more so in the immortalized treated cells relative to controls (Fig. 3, *A* and *B*). Additionally, G:C→C:G transversions were highly elevated in the immortalized treated cells relative to pre-senescent cells. Interestingly, the immortalized control cells also exhibited high frequency of G:C→C:G transversions relative to pre-senescent cells (Fig. 3, *A* and *B*). G:C→C:G transversions have been reported as the most predominant type of mutation in *Trp53* gene in spontaneously immortalized MEF from both WT and *Hupki* mice (harboring a homologous normal human *TP53*) (7). Whole-exome sequencing has also shown a preponderance

of G:C→C:G transversions in spontaneously immortalized MEF (33). Genome-wide analysis of tumors from patients with gingivobuccal oral squamous cell carcinoma has shown a high proportion of G:C→C:G transversions among tobacco users, which, according to the authors, could be ascribed to oxidative DNA damage (34).

The most salient finding of the present study is the observation that A:T→C:G transversions, at a unique sequence-context (*i.e.* flanking purines at the 5′ end of the mutated nucleotide), were the most frequent type of mutation in the immortalized treated cells (23-fold increase in frequency relative to control at T2) (Figs. 3, *A* and *B*, and 5*D*). Importantly, the hallmark A:T→C:G transversions were also enriched in the pre-senescent treated cells, although to a lower extent (2.8-fold increase in frequency relative to control at T2). Oxidative DNA lesions can be formed through two distinct pathways, including 1) direct oxidation of a base (purine/pyrimidine) in DNA and 2) misincorporation of oxidized deoxynucleoside triphosphates (dNTPs) into DNA by DNA polymerase(s) (31, 35, 36). In terms of accumulation of 8-oxodG in DNA, direct oxidation of guanines and incorporation of oxidized guanine nucleotides, 8-hydroxy-2′-deoxyguanosine 5′-triphosphate (8-OH-dGTP) are almost equal contributors (37).

Oxidized dNTPs are generally poor substrates for DNA polymerases although exception exists for certain polymerases (31). For instance, in humans, polymerase η (Polη) incorporates 8-OH-dGTP opposite a template adenine with almost the same efficiency as that of normal 2′-deoxythymidine triphosphate (dTTP) (38). Also, two Y-family DNA polymerases of the archaeon *Sulfolobus solfataricus* sp. (39) and a Y-family polymerase of *E. coli* (DNA Pol IV) (40) have been shown to almost exclusively incorporate 8-OH-dGTP opposite adenine in the DNA template. Such misincorporation leads to A:T→C:G transversion because the oxidized dGTP pairs with an incoming dCMP in the next round of DNA replication (41, 42).

The frequency of spontaneous A:T→C:G transversions has been shown to increase more than 1000-fold over the background in mutT mutant *E. coli*, which is deficient in hydrolyzing 8-OH-dGTP to the monophosphate form and sanitizing the nucleotide pool (29, 43, 44). The extremely high levels of A:T→C:G transversions in the mutT mutant strain are nearly completely suppressed when the cells are cultured in anaerobic conditions, indicating the integral role of oxygen and 8-OH-dGTP in the observed mutagenesis (45). Furthermore, when the cDNA for MutT homolog 1 (MTH1), a human counterpart of *E. coli* MutT, is expressed in mutT mutant cells, the strikingly high rate of spontaneous A:T→C:G mutations reverts to normal (46). Russo *et al.* (47) have demonstrated that overexpression of hMTH1 markedly attenuates the mutation rates in DNA mismatch repair (MMR)–defective mouse and human cells, suggesting that the high spontaneous mutation rates in MMR-defective cells are mostly because of incorporation of oxidized dNTPs into DNA and, less likely, caused by spontaneous replication errors. The authors concluded that incorporation of oxidized purines from the dNTP pool may contribute significantly to the extreme genetic instability of MMR-defective human tumors (47).

In the present study, the preponderant A:T→C:G and G:C→T:A mutations in the immortalized treated cells and, to a lesser extent, in the pre-senescent counterparts as well as spontaneously immortalized untreated cells, are consistent with the previously reported results by others in different model systems (26–29, 35, 38, 40, 43, 44, 46, 47). In our study, the predominant induction of G:C→T:A transversions in the pre-senescent treated cells, which was augmented in the immortalized counterpart cells, is likely to have arisen from error-prone replication bypass of 8-oxodG generated by photosensitization of methylene blue. On the other hand, the overwhelming prevalence of A:T→C:G transversions in the immortalized treated cells and, less so, in the corresponding pre-senescent cells, is likely because of erroneous replication of oxidized guanine nucleosides (8-OHdGTP) produced in the nucleotide pool consequent to methylene blue plus light treatment. A scenario can be envisioned in which the pre-senescent treated cells, which have undergone several rounds of DNA replication, predominantly manifest the signature mutation of 8-oxodG, *i.e.* G:C→T:A transversion. This mutagenic event, leading up to senescence, would be considered short-term effect attributable to the induced oxidative stress. Conversely, the immortalized treated cells, which have had the opportunity to undergo numerous rounds of cell division and DNA replication, preferentially exhaust the oxidized dGTP pool, and give rise primarily to A:T→C:G transversions, in addition to G:C→T:A transversions and other mutations. These characteristic mutations, arising post crisis and after senescence bypass, would constitute long-term effect ascribed to the imposed oxidative stress. Follow-up studies are warranted to investigate the modulation of DNA polymerases and composition of nucleotide pool during cellular senescence and immortalization.

We note that photoactivated methylene blue can also induce oxidized adenine residues, although at much lower level than 8-oxodG (25). For example, treatment of calf thymus DNA with methylene blue plus light produces 8-oxo-7,8-dihydro-2′-deoxyadenosine (8-oxodA) ~29-fold lower than that of 8-oxodG (25). Site-specific mutagenicity studies have demonstrated that 8-oxodA has mutagenic potential (48), although when tested under similar conditions, the mutation frequency of 8-oxodA was, at least, 4-fold lower than that of 8-oxodG (49). Considering the comparatively weaker mutagenicity of 8-oxodA than 8-oxodG and the much lower yield of 8-oxodA in DNA after methylene blue plus light treatment, we may speculate a minor contribution of 8-oxodA to the herein observed elevation of A:T→C:G and A:T→G:C mutation frequencies in the treated cells.

While we underscore the novelty and significance of our findings, we also acknowledge the limitations of our study. For example, interspecies differences in immortalization (4, 5) may influence the generalizability of our findings. Seminal works by others have shown the importance of inactivation of the p53/p19ARF pathway in MEF immortalization (reviewed in Refs. 3–5). Subsequent high throughput screening approaches have identified disruption of additional signaling pathways, including the RAS/MAPK pathway, the AKT pathway, and the JNK pathway, as potential contributors to senescence bypass and immortalization in MEF (3–5). However, immortalization of

human cells in culture is more complex than that of MEF (5). Although disruption of the p53/p14ARF pathway, which corresponds to mouse p53/p19ARF, remains critical, perturbation of the Rb/p16 axis together with reactivation of telomerase are also essential for immortalization of human cells *in vitro* (5, 7). Despite these added complexities, several key components of cellular senescence and immortalization have been retained during evolution and remain functional in both mice and humans (3–5). Thus, the use of MEF *in vitro* or mouse models *in vivo* can provide invaluable information about the underlying mechanisms of senescence and immortalization in human cells (5). Furthermore, in the present study, we have used the *cII* transgene of the Big Blue® MEF as a mutation reporter gene. Transgenes are likely to be transcriptionally inactive, as evidenced by the absence of corresponding mRNA in various tissues of transgenic animals (11). This is relevant because transcription-coupled repair, which preferentially removes DNA lesions from the transcribed strand of endogenous genes, is a key determinant of mutagenesis in mammalian cells (12, 18, 19). The reduced DNA repair capacity of transgenes because of absence of transcription-coupled repair, however, may prove advantageous for mutation detection. This is because transgenes with diminished DNA repair proficiency, are more likely to accumulate promutagenic DNA lesions than endogenous genes (11, 18). This, together with the high copy number of transgenes relative to single copy endogenous genes, may contribute to the high sensitivity of transgenes for mutation detection (12, 18). Altogether, we and others have shown that mutation analysis in transgenes can faithfully recapitulate many aspects of mutagenesis in endogenous genes, although discordant results have also been reported (12, 18, 20). Lastly, DNA damage can result from other ROS, including superoxide radical ($O_2^{-\bullet}$), hydrogen peroxide (H_2O_2), and hydroxyl radical ($^\bullet OH$), which were not analyzed in this study, although $^1O_2$ and $^\bullet OH$ are the only ROS capable of directly damaging DNA (15, 17, 42, 45).

In conclusion, we have generated a compendium of spontaneous and photosensitization-induced mutations in MEF during transition from primary cells through senescence and immortalization. The distinguishing features of photosensitization-induced mutagenesis in the immortalized cells, which are present, at reduced levels, in spontaneously immortalized cells, underscore the importance of oxidative stress in senescence bypass and immortalization. Future investigations are warranted to examine the implications of our findings for human carcinogenesis.

Experimental Procedures

Generation of mouse embryonic fibroblasts

This study was conducted in accordance with the National Institutes of Health's Guide for the Care and Use of Laboratory Animals (50), and all efforts were made to minimize animal suffering. The study was approved by our Institutional Animal Care and Use Committee (IACUC) under the Protocol Number 09012. Primary MEF were isolated from embryos derived from Big Blue® mouse on C57BL/6 genetic background, according to our published protocol (11). Briefly, mouse embryos were harvested *in utero* at 13.5 days of gestation. Following removal of the head and internal organs, individual embryos were placed in a centrifuge tube and incubated with collagenase (Sigma-Aldrich), in DMEM (0.1% v/v) (Irvine Scientific, Santa Ana, CA) for up to 4 h at 37°C. At hourly intervals, the embryo-collagenase mixes were gently centrifuged, pellets were washed with DMEM, and incubation continued in the collagenase solution for the next hour. Upon completion of the digestion, collected cells were transferred to 150-mm Petri dishes containing DMEM, supplemented with 10% FBS (Irvine Scientific) and nonessential amino acids, and subsequently cultured at 37°C. Following 3–4 days of growing, confluent cultures were harvested, and cells were snap frozen (*i.e.* $2–3 \times 10^6$ cells per vial). Upon thawing, MEF cultures were established and expanded for the experiments described below.

Cell culture and treatment

Prior to mutagenicity experiments, a preliminary study was conducted to evaluate the cytotoxicity and DNA-damaging effects of methylene blue plus light, under various treatment conditions. Such preliminary work is conventionally performed to establish a physiologically relevant dose at which a given treatment exerts detectable genotoxic effects without causing excessive cell death. This is important because DNA damage induced by *in vitro* treatment can only be translated into mutation if the treated cells remain viable and proliferate, afterward (11). This allows for the induced DNA damage to evade repair, miscode during translesion synthesis, and upon DNA replication, give rise to mutation (11). *In vitro*, primary Big Blue® MEF undergo cell division every 28–30 h for a few weeks before they reach senescence (*i.e.* passages 5–7). The cells remain in the crisis phase for 3–5 weeks after which single cell clones are formed and spontaneous immortalization occurs (18).

For the preliminary study, early passage Big Blue® MEF were grown as monolayers at ~50–60% confluence in DMEM supplemented with 10% FBS. Prior to treatment, the media were removed, and cells were washed thrice with PBS. Freshly prepared methylene blue (Sigma-Aldrich) dissolved in double-distilled water (stock solution: 10 mM) was added to aliquots of PBS at a final concentration of 2 or 10 μM. Methylene blue–containing PBS aliquots were then added to prewashed MEF culture dishes. For each treatment condition, a set of six MEF cultures was used, including three for cytotoxicity examination and three for DNA damage analysis. The culture dishes containing methylene blue were incubated at 37°C for 30 min in the dark. Subsequently, they were illuminated on ice with visible light for 5, 15, or 45 min (Sylvania, 200 W, A21 SW; OSRAM Sylvania Inc., Wilmington, MA, USA). Throughout the light exposure, culture dishes stayed on a rotating platform (Lazy Susan turntable) at a distance of 10 cm from the bulb. Immediately after the exposure (T0), one half of the cultures, including differently treated cultures and untreated controls (in triplicates), were harvested by trypsinization, pelleted by centrifugation, and preserved at −80°C until DNA damage analysis. The remainder cultures were thoroughly washed with PBS, fed with complete growth medium, and grown in standard cell culture conditions (20% O_2, 5% CO_2, and 37°C) for 24 h.

Subsequently, they were harvested (T1) and subjected to cytotoxicity examination by the trypan blue dye exclusion technique. We set a threshold limit of ≥20% cytotoxicity and a readily detectable level of DNA damage to establish a physiologically relevant dose of methylene blue plus light for our mutagenicity experiment. These threshold criteria are consistent with those used in our previous studies and those by others (12, 18, 19). Upon evaluation of the cytotoxicity and DNA damage in differently treated MEF cultures *versus* controls, we chose a treatment of 2 μM methylene blue plus 5 min light exposure for all mutagenicity experiments (see "Results").

To study ROS-induced mutagenesis before cellular senescence and after immortalization, primary Big Blue® MEF were treated with methylene blue (2 μM) plus light (5-min exposure), as described above. Following the treatment, cells were washed with PBS, fed with DMEM plus FBS, and cultivated in a standard cell culture incubator. The cultures were passed (1:3) when cells reached ~90% confluence, which was, on average, every 3–4 days. Control untreated cultures were prepared and handled similarly, as above. Both the experimental and control cultures were in sets of 12, including 6 for pre-senescence (T2) and 6 for immortalization (T3) analyses. At 8 days posttreatment (T2), one half of the treated and control cultures were harvested, while the remainder underwent further cultivation and passaging, as needed. The T2 harvested cultures (*i.e.* presenescent cells) had undergone several rounds of population doublings, which is a prerequisite for fixation of mutation into the genome (11). After a few weeks of cultivation, the remaining set of cultures entered the crisis phase and became senescent. The senescent cultures were fed twice weekly until they resumed growth and started to form visible clones under microscopy. Single well-isolated clones were selected and reseeded in new dishes for expansion. Dilution cloning was then performed to produce, at least, two single-cell clones, from each expanded culture. Each single-cell clone was further expanded to establish a pure monoclonal population of cells, thus generating an immortalized cell line. The immortalized MEF cell lines derived from the treated and control cultures were harvested and stored at −80°C until further analysis. A schematic diagram of the study design is shown in Fig. 1.

Cleavage assay with DNA repair enzyme and alkaline gel electrophoresis

To detect the characteristic DNA damage induced by methylene blue plus light treatment, we digested the genomic DNA of the treated and control cells with Fpg, a base excision repair enzyme (16, 17), followed by visualization with alkaline gel electrophoresis, as described previously (20) (see supporting information).

cII Mutation analysis

Genomic DNA isolated from the treated and control Big Blue® MEF before senescence and after immortalization was screened for *cII* mutations by the Transpack Packaging Extract kit according to the manufacturer's instructions (Stratagene Corp./Agilent Technologies, Santa Clara, CA, USA). Using the packaging extracts, we recovered the λLIZ shuttle vectors from the genomic DNA and packaged them individually into viable phage particles. The packaged λ phages were then used to infect cultures of G1250 host *E. coli*. The phage-infected G1250 cultures were subsequently plated onto TB1 agar plates and incubated at 24°C for 48 h (*i.e.* selective conditions) to screen for *cII* mutant plaques. To enumerate the total number of plaques screened, dilutions of the corresponding phage-infected G1250 cultures were similarly plated and incubated at 37°C overnight (*i.e.* nonselective conditions). Mutant frequency of the *cII* gene, which represents the mutagenic potency of the test compound(s) or given treatment, is the ratio of the number of mutant plaques (formed in selective conditions) to the total number of plaques screened (WT and mutant *cII* plaques formed in nonselective conditions). To determine the patterns of mutation in the *cII* gene (*i.e.* mutation spectrum) in the treated and control cells, direct DNA sequencing was performed on the verified *cII* mutant plaques, according to our published protocol (18) (see supporting information).

Statistical analysis

Distribution of data was evaluated both visually and by the Shapiro-Wilk test. All results are expressed as median ± S.E. Comparison of mutant frequency data between two different groups was done using the Wilcoxon-Mann-Whitney test. The chi-square test was used to compare the frequency of each specific type of mutation (*e.g.* transition, transversion, indel) between two different groups. All statistical tests were two-sided. Values of $p < 0.05$ were considered statistically significant. All statistical analyses were performed using the R environment for statistical computing, which is a free and open source software.

Data availability

All data are contained within the manuscript.

Acknowledgments—We dedicate this work to the memory of our co-author, colleague, and friend, Steven E. Bates, who was an inspiration to all of us.

Author contributions—A. W. C., S. T., and A. B. formal analysis; A. W. C., S. T., S. E. B., and A. B. validation; A. W. C., S. T., S. E. B., and A. B. investigation; A. W. C., S. T., and A. B. visualization; A. W. C., S. T., S. E. B., and A. B. methodology; S. T. and A. B. funding acquisition; A. B. conceptualization; A. B. resources; A. B. supervision; A. B. writing-original draft; A. B. project administration; A. B. writing-review and editing.

Funding and additional information—This work was supported by NIDCR, National Institutes of Health Grant 1R01DE026043 (to A. B.) and University of California Tobacco-Related Disease Research Program Grants TRDRP-26IR-0015 and TRDRP-28IR-0058 (to A. B.) and TRDRP-26IP-0051 (to S. T.). The content is solely the responsibility of the authors and does not necessarily represent the official views of the National Institutes of Health.

Conflict of interest—The authors declare that they have no conflicts of interest with the contents of this article.

Abbreviations—The abbreviations used are: MEF, mouse embryonic fibroblasts; dTTP, 2′-deoxythymidine triphosphate; 8-OH-dGTP, 8-hydroxy-2′-deoxyguanosine 5′-triphosphate; 8-oxodA, 8-oxo-7,8-dihydro-2′-deoxyadenosine; 8-oxodG, 8-oxo-7,8-dihydro-2′-deoxyguanosine; Fpg, formamidopyrimidine DNA glycosylase; H_2O_2, hydrogen peroxide; indel, insertion and deletion; MMR, DNA mismatch repair; phosphate buffered saline; $O_2^{-\bullet}$, superoxide radical; $^1O_2$, singlet oxygen; $^\bullet$OH, hydroxyl radical; ROS, reactive oxygen species.

References

1. Vogelstein, B., Papadopoulos, N., Velculescu, V. E., Zhou, S., Diaz, L. A., Jr., and Kinzler, K. W. (2013) Cancer genome landscapes. *Science* **339,** 1546–1558 CrossRef Medline
2. Jones, P. A., Issa, J. P., and Baylin, S. (2016) Targeting the cancer epigenome for therapy. *Nat. Rev. Genet.* **17,** 630–641 CrossRef Medline
3. Muñoz-Espín, D., and Serrano, M. (2014) Cellular senescence: From physiology to pathology. *Nat. Rev. Mol. Cell Biol.* **15,** 482–496 CrossRef Medline
4. Gorgoulis, V., Adams, P. D., Alimonti, A., Bennett, D. C., Bischof, O., Bishop, C., Campisi, J., Collado, M., Evangelou, K., Ferbeyre, G., Gil, J., Hara, E., Krizhanovsky, V., Jurk, D., Maier, A. B., *et al.* (2019) Cellular senescence: Defining a path forward. *Cell* **179,** 813–827 CrossRef Medline
5. Odell, A., Askham, J., Whibley, C., and Hollstein, M. (2010) How to become immortal: Let MEFs count the ways. *Aging* **2,** 160–165 CrossRef Medline
6. Hayflick, L., and Moorhead, P. S. (1961) The serial cultivation of human diploid cell strains. *Exp. Cell Res.* **25,** 585–621 CrossRef Medline
7. Whibley, C., Odell, A. F., Nedelko, T., Balaburski, G., Murphy, M., Liu, Z., Stevens, L., Walker, J. H., Routledge, M., and Hollstein, M. (2010) Wild-type and Hupki (human p53 knock-in) murine embryonic fibroblasts: p53/ARF pathway disruption in spontaneous escape from senescence. *J. Biol. Chem.* **285,** 11326–11335 CrossRef Medline
8. Tommasi, S., Zheng, A., Weninger, A., Bates, S. E., Li, X. A., Wu, X., Hollstein, M., and Besaratinia, A. (2013) Mammalian cells acquire epigenetic hallmarks of human cancer during immortalization. *Nucleic Acids Res.* **41,** 182–195 CrossRef Medline
9. Busuttil, R. A., Rubio, M., Dollé, M. E., Campisi, J., and Vijg, J. (2003) Oxygen accelerates the accumulation of mutations during the senescence and immortalization of murine cells in culture. *Aging Cell* **2,** 287–294 CrossRef Medline
10. Parrinello, S., Samper, E., Krtolica, A., Goldstein, J., Melov, S., and Campisi, J. (2003) Oxygen sensitivity severely limits the replicative lifespan of murine fibroblasts. *Nat. Cell Biol.* **5,** 741–747 CrossRef Medline
11. Besaratinia, A., Zheng, A., Bates, S. E., and Tommasi, S. (2018) Mutation analysis in cultured cells of transgenic rodents. *Int. J. Mol. Sci.* **19,** 262 CrossRef Medline
12. White, P. A., Luijten, M., Mishima, M., Cox, J. A., Hanna, J. N., Maertens, R. M., and Zwart, E. P. (2019) In vitro mammalian cell mutation assays based on transgenic reporters: A report of the International Workshop on Genotoxicity Testing (IWGT). *Mutat. Res.* **847,** 403039 CrossRef Medline
13. Epe, B., Hegler, J., and Wild, D. (1989) Singlet oxygen as an ultimately reactive species in *Salmonella typhimurium* DNA damage induced by methylene blue/visible light. *Carcinogenesis* **10,** 2019–2024 CrossRef Medline
14. Floyd, R. A., West, M. S., Eneff, K. L., and Schneider, J. E. (1989) Methylene blue plus light mediates 8-hydroxyguanine formation in DNA. *Arch. Biochem. Biophys.* **273,** 106–111 CrossRef Medline
15. Tuite, E. M., and Kelly, J. M. (1993) Photochemical interactions of methylene blue and analogues with DNA and other biological substrates. *J. Photo. Photobiol. B* **21,** 103–124 CrossRef Medline
16. Boiteux, S., Gajewski, E., Laval, J., and Dizdaroglu, M. (1992) Substrate specificity of the *Escherichia coli* Fpg protein (formamidopyrimidine-DNA glycosylase): Excision of purine lesions in DNA produced by ionizing radiation or photosensitization. *Biochemistry* **31,** 106–110 CrossRef Medline
17. Cadet, J., Ravanat, J. L., Martinez, G. R., Medeiros, M. H., and Di Mascio, P. (2006) Singlet oxygen oxidation of isolated and cellular DNA: Product formation and mechanistic insights. *Photochem. Photobiol.* **82,** 1219–1225 CrossRef Medline
18. Besaratinia, A., and Tommasi, S. (2018) The lambda select cII mutation detection system. *J. Vis. Exp.* **2018,** 57510 CrossRef Medline
19. Kucab, J. E., Zou, X., Morganella, S., Joel, M., Nanda, A. S., Nagy, E., Gomez, C., Degasperi, A., Harris, R., Jackson, S. P., Arlt, V. M., Phillips, D. H., and Nik-Zainal, S. (2019) A compendium of mutational signatures of environmental agents. *Cell* **177,** 821–836.e816 CrossRef Medline
20. Besaratinia, A., Kim, S. I., and Pfeifer, G. P. (2008) Rapid repair of UVA-induced oxidized purines and persistence of UVB-induced dipyrimidine lesions determine the mutagenicity of sunlight in mouse cells. *FASEB J.* **22,** 2379–2392 CrossRef Medline
21. Duncan, B. K., and Miller, J. H. (1980) Mutagenic deamination of cytosine residues in DNA. *Nature* **287,** 560–561 CrossRef Medline
22. Tchou, J., Bodepudi, V., Shibutani, S., Antoshechkin, I., Miller, J., Grollman, A. P., and Johnson, F. (1994) Substrate specificity of Fpg protein. Recognition and cleavage of oxidatively damaged DNA. *J. Biol. Chem.* **269,** 15318–15324 Medline
23. Coste, F., Ober, M., Carell, T., Boiteux, S., Zelwer, C., and Castaing, B. (2004) Structural basis for the recognition of the FapydG lesion (2,6-diamino-4-hydroxy-5-formamidopyrimidine) by formamidopyrimidine-DNA glycosylase. *J. Biol. Chem.* **279,** 44074–44083 CrossRef Medline
24. Mellish, K. J., Cox, R. D., Vernon, D. I., Griffiths, J., and Brown, S. B. (2002) In vitro photodynamic activity of a series of methylene blue analogues. *Photochem. Photobiol.* **75,** 392–397 CrossRef Medline
25. Singh, R., Teichert, F., Verschoyle, R. D., Kaur, B., Vives, M., Sharma, R. A., Steward, W. P., Gescher, A. J., and Farmer, P. B. (2009) Simultaneous determination of 8-oxo-2′-deoxyguanosine and 8-oxo-2′-deoxyadenosine in DNA using online column-switching liquid chromatography/tandem mass spectrometry. *Rapid Commun. Mass Spectrom.* **23,** 151–160 CrossRef Medline
26. Wood, M. L., Dizdaroglu, M., Gajewski, E., and Essigmann, J. M. (1990) Mechanistic studies of ionizing radiation and oxidative mutagenesis: Genetic effects of a single 8-hydroxyguanine (7-hydro-8-oxoguanine) residue inserted at a unique site in a viral genome. *Biochemistry* **29,** 7024–7032 CrossRef Medline
27. Cheng, K. C., Cahill, D. S., Kasai, H., Nishimura, S., and Loeb, L. A. (1992) 8-Hydroxyguanine, an abundant form of oxidative DNA damage, causes G→T and A→C substitutions. *J. Biol. Chem.* **267,** 166–172 Medline
28. Tudek, B., Laval, J., and Boiteux, S. (1993) SOS-independent mutagenesis in lacZ induced by methylene blue plus visible light. *Mol. Gen. Genet.* **236,** 433–439 CrossRef Medline
29. Michaels, M. L., Cruz, C., Grollman, A. P., and Miller, J. H. (1992) Evidence that MutY and MutM combine to prevent mutations by an oxidatively damaged form of guanine in DNA. *Proc. Natl. Acad. Sci. U.S.A.* **89,** 7022–7025 CrossRef Medline
30. Pavlov, Y. I., Minnick, D. T., Izuta, S., and Kunkel, T. A. (1994) DNA replication fidelity with 8-oxodeoxyguanosine triphosphate. *Biochemistry* **33,** 4695–4701 CrossRef Medline
31. Nohmi, T., Kim, S. R., and Yamada, M. (2005) Modulation of oxidative mutagenesis and carcinogenesis by polymorphic forms of human DNA repair enzymes. *Mutat. Res.* **591,** 60–73 CrossRef Medline
32. Henderson, P. T., Delaney, J. C., Muller, J. G., Neeley, W. L., Tannenbaum, S. R., Burrows, C. J., and Essigmann, J. M. (2003) The hydantoin lesions formed from oxidation of 7,8-dihydro-8-oxoguanine are potent sources of replication errors in vivo. *Biochemistry* **42,** 9257–9262 CrossRef Medline
33. Olivier, M., Weninger, A., Ardin, M., Huskova, H., Castells, X., Vallée, M. P., McKay, J., Nedelko, T., Muehlbauer, K. R., Marusawa, H., Alexander, J., Hazelwood, L., Byrnes, G., Hollstein, M., and Zavadil, J. (2014) Modelling mutational landscapes of human cancers in vitro. *Sci. Rep.* **4,** 4482 CrossRef Medline
34. India Project Team of the International Cancer Genome Consortium. (2013) Mutational landscape of gingivo-buccal oral squamous cell

carcinoma reveals new recurrently-mutated genes and molecular subgroups. *Nat. Commun.* **4,** 2873 CrossRef Medline
35. Inoue, M., Kamiya, H., Fujikawa, K., Ootsuyama, Y., Murata-Kamiya, N., Osaki, T., Yasumoto, K., and Kasai, H. (1998) Induction of chromosomal gene mutations in *Escherichia coli* by direct incorporation of oxidatively damaged nucleotides. New evaluation method for mutagenesis by damaged DNA precursors *in vivo*. *J. Biol. Chem.* **273,** 11069–11074 CrossRef Medline
36. Hidaka, K., Yamada, M., Kamiya, H., Masutani, C., Harashima, H., Hanaoka, F., and Nohmi, T. (2008) Specificity of mutations induced by incorporation of oxidized dNTPs into DNA by human DNA polymerase eta. *DNA Repair* **7,** 497–506 CrossRef Medline
37. Tajiri, T., Maki, H., and Sekiguchi, M. (1995) Functional cooperation of MutT, MutM and MutY proteins in preventing mutations caused by spontaneous oxidation of guanine nucleotide in *Escherichia coli*. *Mutat. Res.* **336,** 257–267 CrossRef Medline
38. Shimizu, M., Gruz, P., Kamiya, H., Masutani, C., Xu, Y., Usui, Y., Sugiyama, H., Harashima, H., Hanaoka, F., and Nohmi, T. (2007) Efficient and erroneous incorporation of oxidized DNA precursors by human DNA polymerase η. *Biochemistry* **46,** 5515–5522 CrossRef Medline
39. Shimizu, M., Gruz, P., Kamiya, H., Kim, S. R., Pisani, F. M., Masutani, C., Kanke, Y., Harashima, H., Hanaoka, F., and Nohmi, T. (2003) Erroneous incorporation of oxidized DNA precursors by Y-family DNA polymerases. *EMBO Rep.* **4,** 269–273 CrossRef Medline
40. Yamada, M., Nunoshiba, T., Shimizu, M., Gruz, P., Kamiya, H., Harashima, H., and Nohmi, T. (2006) Involvement of Y-family DNA polymerases in mutagenesis caused by oxidized nucleotides in *Escherichia coli*. *J. Bacteriol.* **188,** 4992–4995 CrossRef Medline
41. Michaels, M. L., and Miller, J. H. (1992) The GO system protects organisms from the mutagenic effect of the spontaneous lesion 8-hydroxyguanine (7,8-dihydro-8-oxoguanine). *J. Bacteriol.* **174,** 6321–6325 CrossRef Medline
42. Kasai, H. (2002) Chemistry-based studies on oxidative DNA damage: Formation, repair, and mutagenesis. *Free Radic. Biol. Med.* **33,** 450–456 Medline
43. Maki, H., and Sekiguchi, M. (1992) MutT protein specifically hydrolyses a potent mutagenic substrate for DNA synthesis. *Nature* **355,** 273–275 CrossRef Medline
44. Sakumi, K., Furuichi, M., Tsuzuki, T., Kakuma, T., Kawabata, S., Maki, H., and Sekiguchi, M. (1993) Cloning and expression of cDNA for a human enzyme that hydrolyzes 8-oxo-dGTP, a mutagenic substrate for DNA synthesis. *J. Biol. Chem.* **268,** 23524–23530 Medline
45. Sakai, A., Nakanishi, M., Yoshiyama, K., and Maki, H. (2006) Impact of reactive oxygen species on spontaneous mutagenesis in *Escherichia coli*. *Genes Cells* **11,** 767–778 CrossRef Medline
46. Furuichi, M., Yoshida, M. C., Oda, H., Tajiri, T., Nakabeppu, Y., Tsuzuki, T., and Sekiguchi, M. (1994) Genomic structure and chromosome location of the human mutT homologue gene MTH1 encoding 8-oxo-dGTPase for prevention of A:T to C:G transversion. *Genomics* **24,** 485–490 CrossRef Medline
47. Russo, M. T., Blasi, M. F., Chiera, F., Fortini, P., Degan, P., Macpherson, P., Furuichi, M., Nakabeppu, Y., Karran, P., Aquilina, G., and Bignami, M. (2004) The oxidized deoxynucleoside triphosphate pool is a significant contributor to genetic instability in mismatch repair-deficient cells. *Mol. Cell. Biol.* **24,** 465–474 CrossRef Medline
48. Kamiya, H., Miura, H., Murata-Kamiya, N., Ishikawa, H., Sakaguchi, T., Inoue, H., Sasaki, T., Masutani, C., Hanaoka, F., and Nishimura, S. and (1995) 8-Hydroxyadenine (7,8-dihydro-8-oxoadenine) induces misincorporation in *in vitro* DNA synthesis and mutations in NIH 3T3 cells. *Nucleic Acids Res.* **23,** 2893–2899 CrossRef Medline
49. Tan, X., Grollman, A. P., and Shibutani, S. (1999) Comparison of the mutagenic properties of 8-oxo-7,8-dihydro-2′-deoxyadenosine and 8-oxo-7,8-dihydro-2′-deoxyguanosine DNA lesions in mammalian cells. *Carcinogenesis* **20,** 2287–2292 CrossRef Medline
50. National Research Council. (2011) *Guide for the Care and Use of Laboratory Animals*, 8th ed., National Academies Press, Washington, DC
51. Besaratinia, A., Yoon, J.-I., Schroeder, C., Bradforth, S. E., Cockburn, M., and Pfeifer, G. P. (2011) Wavelength dependence of ultraviolet radiation-induced DNA damage as determined by laser irradiation suggests that cyclobutane pyrimidine dimers are the principal DNA lesions produced by terrestrial sunlight. *FASEB J.* **25,** 3079–3091 CrossRef Medline
52. Boiteux, S., O'Connor, T. R., and Laval, J. (1987) Formamidopyrimidine-DNA glycosylase of *Escherichia coli*: Cloning and sequencing of the fpg structural gene and overproduction of the protein. *EMBO J.* **6,** 3177–3183 CrossRef Medline
53. Jakubczak, J. L., Merlino, G., French, J. E., Muller, W. J., Paul, B., Adhya, S., and Garges, S. (1996) Analysis of genetic instability during mammary tumor progression using a novel selection-based assay for in vivo mutations in a bacteriophage lambda transgene target. *Proc. Natl. Acad. Sci. U. S. A.* **93,** 9073–9078 CrossRef Medline
54. Lambert, I. B., Singer, T. M., Boucher, S. E., and Douglas, G. R. (2005) Detailed review of transgenic rodent mutation assays. *Mutat. Res.* **590,** 1–280 CrossRef Medline
55. Herskowitz, I., and Hagen, D. (1980) The lysis-lysogeny decision of phage lambda: Explicit programming and responsiveness. *Ann. Rev. Genet.* **14,** 399–445 CrossRef Medline
56. Agilent Technologies. λ *Select-cII Mutation Detection System for Big Blue Rodents. Instruction Manual*, Revision B.0, Stratagene Products Division, Agilent Technologies, La Jolla, CA

Spontaneous and photosensitization-induced mutations in primary mouse cells transitioning through senescence and immortalization

Andrew W. Caliri, Stella Tommasi, Steven E. Bates and Ahmad Besaratinia

J. Biol. Chem. 2020, 295:9974-9985.
doi: 10.1074/jbc.RA120.014465 originally published online June 2, 2020